Multi-robot Source Seeking and Field Reconstruction of Spatial-temporal Varying Fields

Deepak Talwar, Thinh Lu, Divyam Sobti, and Wencen Wu*
Computer Engineering Department
San José State University
San José, CA, USA

Emails: deepaktalwardt@gmail.com, {thinh.lu, divyam.sobti, wencen.wu}@sjsu.edu

Abstract—To effectively respond to environmental disasters, real-time monitoring and pollution control rely heavily on the ability to estimate, predict, and reconstruct constantly changing environmental conditions across different locations. In this research, we develop a multi-robot source-seeking and field reconstruction framework that enables a multi-robot group to detect multiple sources within a spatial-temporal varying field and reconstruct the field in real time. The strategy consists of two parts: source seeking and field reconstruction. The sourceseeking part features a gradient-based source-seeking controller that directs the multi-robot group toward local sources and a destination selection algorithm that navigates the multi-robot formation beyond the local maximal. The field reconstruction part reconstructs the spatial-temporal varying field in real time using the limited measurements taken by the robots. We validate the strategy in simulations.

Index Terms—mobile sensor networks, field reconstruction, source seeking.

I. INTRODUCTION

Understanding complex environmental processes such as pollution evolution, salinity distribution, and wildfire propagation, is crucial for environmental monitoring tasks. These processes are often governed by partial differential equations (PDEs) due to the spatial temporal-varying states [1]. For example, the advection-diffusion equation can model the dynamics of smoke plumes in a given region over time, where the advection term describes the movement of the smoke plume driven by wind velocity, and the diffusion term represents the spatial dispersion of the smoke from higher to lower concentration areas. Accurate estimation, prediction, and real-time reconstruction of spatial-temporal varying fields are vital for effective environmental monitoring and disaster management [2].

The field reconstruction typically consists of two primary challenges: identifying the unknown parameters within the governing PDEs and estimating the state of the concentration field across a selected spatial domain. The conventional approach of deploying extensive static sensor networks is often prohibitive due to the high costs associated with covering large areas. An alternative approach utilizes a few mobile robots with sensors to explore vast areas, gathering data as they move along their path[3], [4]. Yet, the spatial-temporal variability of

field concentrations and the scarcity of sensor measurements pose significant challenges.

In recent years, various approaches have been developed to solve the problem of parameter identification [5], [6], [7] and field reconstruction using mobile sensor networks. Among these, In [8], [9], a cooperative Kalman filter combined with a recursive least square (RLS) method has been developed to provide real-time parameter identification of advectiondiffusion fields, enabling field reconstruction via PDEs. For effective real-time field reconstruction, the accuracy of state estimation is significantly influenced by the trajectories navigated by mobile robots. Accordingly, it is imperative to strategically direct these robots along paths that are rich in information. In works [4] and [10], the authors incorporated the dynamics of mobile robots into the dynamics of the field. The optimization of these paths predominantly focuses on minimizing mapping errors. Such an approach may lead to solutions that converge on local optima, overlook areas of high concentration, and are inadequate for reconstructing complex fields with multiple sources of concentration. In [11], the authors developed a path-planning method that employs geometric reinforcement learning for navigating through areas that exhibit multiple high-concentration zones. However, this method needs to specify a target location within the area for search purposes, a task that presents challenges in fields characterized by intricate concentration distributions.

In this research, we propose a multi-robot source-seeking and field reconstruction framework that allows a multi-robot group to identify multiple sources in a spatial-temporal varying field and reconstruct the field in real time. The strategy consists of two parts: source seeking and field reconstruction. The source-seeking part features a gradient-based controller that directs the multi-robot group toward local maximums corresponding to sources in a field, and a destination selection algorithm that allows the multi-robot group to jump out of a local maximal and keep exploring the unvisited area of the field to maximize coverage [12]. The field reconstruction part reconstructs the spatial-temporal varying field in real time using the limited measurements collected by the robots. We validate the strategy in simulations in a spatial-temporal varying field and compare the field reconstruction errors with baseline strategies when the multi-robot group only follows random or lawn-mowing trajectories. This strategy promotes exploration when the measured field concentration encounters

a local maximum, thereby enhancing the ability to recreate fields with multiple sources.

The remaining part of the paper is organized as follows. The problem is formulated in Section II. Section III presents the proposed algorithm and IV demonstrates the simulation results and analysis. Section V concludes the paper and discusses future work.

II. PROBLEM FORMULATION

In this section, we introduce the problem formulation of the field reconstruction task using a formation of mobile robots. The field is represented as a linear combination of multiple advection-diffusion equations.

A. Advection-Diffusion Fields

Numerous processes that vary both spatially and temporally can be represented as two-dimensional (2D) partial differential equations within a certain area Ω , as follows:

$$\frac{\partial z}{\partial t}(r,t) = \mathcal{F}(z(r,t), \nabla z(r,t), \nabla^2 z(r,t)), \quad r \in \Omega, \quad (1)$$

where Ω represents the area of interest, z(r,t) is the field value of a sptail-temporal-varying scalar field at location z at time t, $\nabla z(r,t)$ is the gradient at location r, $\nabla^2 z(r,t)$) represents the Laplacian matrix at location r, and $\mathcal{F}(\cdot)$ is an unknown possibily nonlinear function. In practice, many processes are governed by advection-diffusion phenomena, which can be represented by the advection-diffusion equation as

$$\frac{\partial z}{\partial t}(r,t) = \theta \nabla^2 z(r,t) + \mathbf{v} \nabla z(r,t), \quad r \in \Omega, \tag{2}$$

where $\theta>0$ represents the diffusion coefficient and ${\bf v}$ is the advection coefficient. In this work, the diffusion coefficient is assumed to be a low value, allowing for the presumption that the field exhibits negligible turbulence. We further assume that the advection coefficient ${\bf v}$ is constant throughout space and time in domain Ω . This is generally true for environmental processes that occur over a large area.

We consider an area Ω with the size being significantly larger than the size of the robots. This is a common scenario in real-life environmental monitoring missions. Given this setting, the boundary of the area can be modeled as a flat surface. Therefore, we can assume initial and Dirichlet boundary conditions for the field as[2]:

$$z(r,0) = z_0(r),$$

$$z(r,t) = 0, r \in \partial\Omega.$$
(3)

In this work, we assume that the field of interest $z_0(r, t=0)$ is a linear combination of several advection-diffusion equations (2), thus, forming a non-linear surface with with multiple sources.

B. Mobile Sensor Robots

We employ N mobile robots equipped with sensors in the field. For simplicity, we consider the first-order dynamics of the robots, i.e., $\dot{r}_i(t) = u_i(t)$, i = 1, 2, 3, ..., N, where $r_i(t) \in \mathbb{R}^2$ is the location of the *i*th robot in the area Ω , and

 $u_i(t) \in \mathbb{R}^2$ represents the velocity control for the ith robot at time t. Each robot is able to determine its location within Ω at discrete time intervals k and to communicate its position r_i^k to its peers. By collating the positions of all robots, the center of the formation r_c^k at discrete time k is calculated as $r_c^k = \frac{1}{N} \sum_{i=1}^N r_i^k$. Moreover, every robot carries sensors to measure the field value. The measurement made by the ith robot at time k is represented by the following equation:

$$p(r_i^k, k) = z(r_i^k, k) + n_i, \tag{4}$$

in which n_i is considered to be independent and identically distributed Gaussian noise.

To assist in the development of the proposed algorithm, a dynamic view-scope $\Gamma(t)$ for the robot formation is introduced. The view-scope Γ at any moment t encompasses the portion of the area Ω within the polygon defined by the positions of the sensing robots, as depicted in Fig. 1. Although the sensing robots are restricted to measuring and sharing concentration data only from their immediate locations, the field values $z(r,t), \ r \in \Gamma(t)$ can be derived by interpolating these measured values.

Additionally, the formation controller and the cooperative Kalman filter developed in [13] are employed to control the robot group to maintain a desired formation and produce estimates of the field value $z(r_c,t)$ and field gradient $\nabla z(r_c,t)$ along the trajectory of the formation center r_c . We further assume that the diffusion parameter of the field (2) can be estimated using algorithms developed in [9]. Given that the robots are coordinated to maintain a formation, the planning and control task is simplified to planning the path and designing the controller for the formation center

With the above settings, the task of source-seeking and field reconstruction reduces to the following two steps:

- 1) Source detection. The concentration function z(r,t) can be thought of as a linear combination of concentration values produced by said sources. Thus, identifying the sources is critical in field reconstruction.
- 2) Field reconstruction. Estimate the state, i.e. field concentration value in the area Ω to reconstruct the field.

III. PROPOSED ALGORITHM

In this section, we introduce the source-seeking and field reconstruction framework. The source-seeking part contains a gradient-based controller and a destination selection algorithm to allow the multi-robot formation to identify multiple sources, and the field reconstruction part uses the knowledge of the advection-diffusion equation to propagate field concentration values with measurements provided by mobile robots.

A. Gradient-based Source-Seeking

As mentioned in the problem formulation, we employ the formation controller [13] to control the multi-robot group to remain in a desired formation, thus, the source-seeking controller can be just designed for the formation center r_c . Additionally, we use the cooperative Kalman filter developed in [9] to estimate the field gradient along the formation center

while the formation is moving in the field. The formation center can be controlled as

$$\dot{r}_c = v_c \frac{\nabla z(r_c, t)}{||\nabla z(r_c, t)||},\tag{5}$$

where v_c is the constant speed specified for the formation center. With the gradient information, the formation center can be controlled to move toward a local source corresponding to a local maximum in the field.

B. Destination Selection for Further Exploration

Upon reaching a local maximum within the field, it's crucial to motivate the mobile robot formation to venture into unexplored segments of the domain. Given that many environmental phenomena may exhibit areas of high concentration, leading to complex concentration profiles, a comprehensive exploration by the formation is essential for accurate field reconstruction. To address this, we introduce an algorithm designed to foster exploration away from previously visited regions within the field domain Ω . This algorithm determines a destination $r_d \in \Omega$ towards which the formation will move toward, subsequently resuming navigation along gradient paths.

The algorithm for choosing destinations adheres to specific criteria:

- 1) The chosen destination should be distinct from and beyond the scope of areas already explored.
- 2) A preference should be given to regions within Ω that remain unexplored.
- The destination must be sufficiently remote to enable the gradient-based controller to detect new sources if they exist.

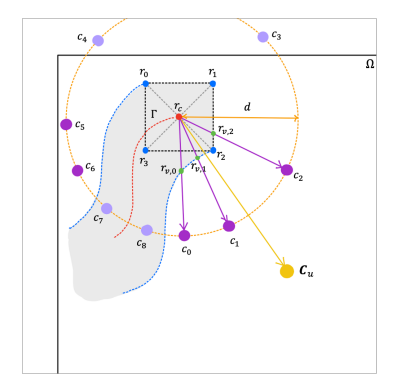


Fig. 1. Illustration demonstrating the destination selection algorithm.

We initiate the algorithm by defining a distance d that establishes how far we aim for the selected destination to be from the current formation center (r_c) . Using the distance d, we construct a set D comprising potential destinations. From this set, any location that falls outside of the domain Ω or has been previously visited is excluded, resulting in a refined set D_u of unexplored candidate locations. The subsequent step involves selecting a destination from D_u that aligns with our established criteria. For each candidate c_i within D_u , we assign a weight w_i according to the equation:

$$w_i = \text{similarity}(r_c - \mathbf{C}_u, c_i - \mathbf{C}_u) \|c_i - r_{v,i}\|_2, \ \forall c_i \in D_u, \ (6)$$

where $r_{v,i}$ represents the nearest previously visited location to c_i in the direction of r_c , \mathbf{C}_u denotes the centroid of the unvisited areas U within Ω , and similarity is defined by the cosine similarity between two vectors. This similarity measure calculates the cosine of the angle between two n-dimensional vectors \mathbf{A} and \mathbf{B} :

similarity(
$$\mathbf{A}, \mathbf{B}$$
) = $\frac{\mathbf{A} \cdot \mathbf{B}}{\|\mathbf{A}\| \|\mathbf{B}\|}$. (7)

Thus, the similarity $(r_c - \mathbf{C}_u, c_i - \mathbf{C}_u)$ in Equation (6) calculates the cosine of the angle between $r_c - \mathbf{C}_u$ and $c_i - \mathbf{C}_u$. The former one represents the vector connecting the formation center's current location and the centroid of the regions that have not been visited. The latter one represents the vector connecting the ith candidate and the centroid of the regions that have not been visited. The weight w_i will be used in the random sampling for candidate locations. Given this design, consequently, candidates in the direction of C_u receive higher weighting than candidates in the opposite direction from C_u . In addition, the $||c_i - r_{v,i}||_2$ term in Equation (6) calculates the Euclidean distance between the ith candidate c_i and the closest visited location to it in the direction of r_c . Therefore, for those candidates in the direction of C_u , candidates farther from the visited regions are prioritized. Fig. 1 demonstrates the concept behind the proposed algorithm. In this diagram, the mobile robots r_0, r_1, r_2 , and r_3 are shown in formation, with r_c indicating the center of this formation. The region enclosed by the black dashed lines represents the view-scope Γ . The yellow point \mathbf{C}_u signifies the centroid of areas within Ω that have yet to be explored. The area shaded in gray indicates territories that the formation has already traversed. The dashed orange circle encompasses all points at distance d from r_c , creating the potential destination set D. Selected examples from this set, marked as c_i , where i = 0, 1, 2...8, are shown. From these examples, c_3 and c_4 are excluded because they fall outside the domain Ω , and c_7 and c_8 are disregarded as they are within previously explored areas. Consequently, c_0, c_1, c_2, c_5 , and c_6 are included in set D_u as viable destination candidates. The points $r_{v,0}, r_{v,1}$, and $r_{v,2}$ represent the nearest previously visited locations towards r_c for the candidates c_0, c_1 , and c_2 , respectively. In this instance, c_1 is deemed most likely to be chosen as it directs towards C_u .

To utilize the calculated weights for randomly drawing destinations, they are converted into a probability distribution through exponentiation and normalization as follows:

$$\Pr(c_i) = \frac{e^{w_i}}{\sum_{i=0}^{|D_u|} e^{w_i}},$$
(8)

where the exponentiation amplifies the distinction between more and less preferable candidates. This probability distribution then facilitates the random selection of a destination, effectively integrating both distance and orientation preferences into the decision-making process. The methodology for implementing this algorithm is detailed in the subsequent algorithm description in Algorithm 1.

After the destination has been chosen, the formation will resume the source-seeking by employing the gradient-based controller in (5).

Algorithm 1 Destination Selection Algorithm

```
Require: r_c, d, U
   D \leftarrow candidate destinations d distance away from r_c
   D_u = []
   for c_i \in D do
      if c_i \in \Omega and c_i \in U then
          D_u.insert(c_i)
      end if
   end for
  \mathbf{C}_u = \frac{1}{|U|} \sum_{i=0}^{|U|} r_i, weights = []
for c_i \in D_u do
      r_{v,i} \leftarrow trace ray from c_i to r_c to find first visited location proposed algorithm.
      w = \text{similarity}(r_c - \mathbf{C}_u, c_i - \mathbf{C}_u) \|c_i - r_{v,i}\|_2
      weights.insert(w)
end for
probabilities = [] {Initialize probabilities array}
for w_i \in \text{weights do}
      p = \frac{\bar{e}^{w_i}}{\sum_{i=0}^{|D_u|} e^{w_i}} probabilities.insert(p)
end for
idx \leftarrow randomly drawn index with probabilities
return D_u[idx] = 0
```

C. Advection-Diffusion Field Reconstruction

To reconstruct the field, we discretize Equation (2) over space and time. In Fig. 2, we illustrate a 3×3 area of the discretized field, where N=4 robots are placed symmetrically. Using the finite difference method, the Equation (2) can be discretized as:

$$\frac{z(r_0, k+1) - z(r_0, k)}{t_s} = \theta \left[\frac{z(r_2, k) + z(r_4, k) - 2z(r_0, k)}{\Delta r_x^2} + \frac{z(r_1, k) + z(r_3, k) - 2z(r_0, k)}{\Delta r_y^2} + \mathbf{v}^T \nabla z(r_0, k) + e(r_0, k), \right]$$
(9)

where k is the discretized time step, t_s is the sampling interval and $e(r_0, k)$ accounts for the approximation error. Assuming square grid cells, i.e., $\Delta r_x = \Delta r_y$, Equation (9) simplifies to the following.

$$\frac{z(r_0, k+1) - z(r_0, k)}{t_s} = \theta \frac{\sum_{i=1}^4 z(r_i, k) - 4z(r_0, k)}{\Delta r_x^2} + \mathbf{v}^T \nabla z(r_0, k) + e(r_0, k).$$
(10)

With given advection and diffusion coefficients \mathbf{v} and θ , the advection-diffusion field can be simulated using Equation (10) for each grid $r_0 \in \Omega$.

At every time step k, we derive estimates of the field concentration values within the view-scope, denoted as $\hat{z}(r,k)$ where $r \in \Gamma(k)$. Thus, at each time step k, it becomes possible to fill in the estimated concentration values within the current view-scope and utilize Equation (10) to propagate the field's state. This methodology facilitates the reconstruction of the field utilizing merely the sparse measurements collected along the paths of the robots.

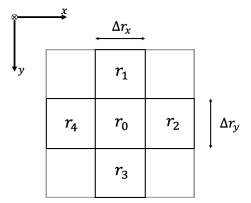


Fig. 2. A 3×3 section of the discretized advection-diffusion field.

IV. SIMULATION RESULTS

In this section, we present the simulation results of the proposed algorithm.

We generate a simulated spatial-temporal varying field, which is a linear combination of two advection-diffusion equations, with the initial sources located at [20, 30] and [80, 70]. Both fields are characterized by an advection coefficient (v = 0) and a diffusion coefficient ($\theta = 0.1$). A group of four mobile robots is controlled in a symmetric formation and initiates the exploration at [10, 10]. Following the strategy described in III, the formation initially engages in source-seeking. Upon encountering a source, it follows the destination selection algorithm to keep exploring the field and move toward another source in the lower right corner. The robots' collected measurements facilitate real-time field reconstruction. Figure. 3 illustrates the trajectory of the formation center in the simulated field (left) and the reconstructed field (right). The black dots correspond to the source-seeking mode and the red dots correspond to the field exploration mode. The figures in the right column show the field reconstruction results at different time steps. The multi-robot formation stops when it reaches the second source. Figure. 4 demonstrates the concentration value of the field measured at the formation center along its trajectory. We can observe from the figure that there are two peaks in the figure, representing the two sources. With the field's diffusing nature, a gradual decrease in concentration values in the vicinity of this source is observed afterward.

We use the mapping error to quantify the reconstruction's accuracy. We define the mapping error at time step k as:

$$e_M(k) = \sum_{r \in \Omega} |z(r, k) - \hat{z}(r, k)|,$$
 (11)

where, z(r,k) is the true field value at k and $\hat{z}(r,k)$ represents the estimated field value in the reconstructed field at time step k. The goal of field reconstruction is to design a path for the robot formation to efficiently collect data so that the mapping error can be gradually decreased. Fig. 5 shows the mapping errors while the multi-robot formation is moving in the field.

To demonstrate the effectiveness of the proposed strategy, we replaced the trajectory planning strategy, i.e., gradient-based source-seeking and destination-selection algorithms, with two baseline approaches: random trajectory and lawn-mowing trajectory. Fig. 5 illustrates the simulation results in the same field with different colors corresponding to different strategies: red for gradient, green for lawnmowing, and black for random. It can be clearly observed that our proposed strategy outperforms the other two.

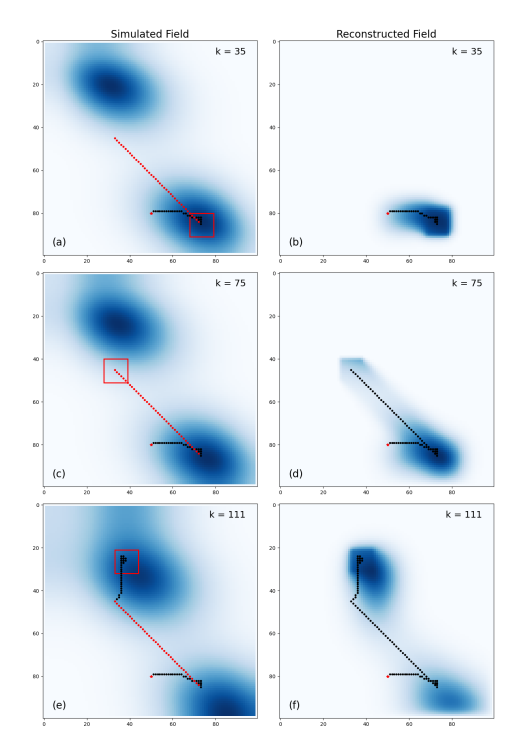


Fig. 3. source-seeking (black) and exploration (red) operation of the robot formation during field reconstruction

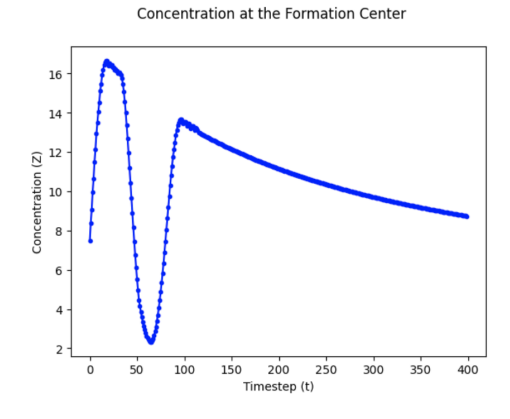


Fig. 4. The concentration at the formation center along the trajectory.

V. CONCLUSIONS AND FUTURE WORK

In this study, we developed and validated a multi-robot field reconstruction strategy to reconstruct spatial-temporal varying fields that are governed by multiple advection-diffusion equations. Central to our approach is a destination-selection algorithm that empowers a coordinated multi-robot formation to navigate beyond local maxima, ensuring thorough exploration of previously uncharted territories. This capability is pivotal for the accurate and efficient reconstruction of dynamically varying fields. In the future, we plan to integrate the strategy with advanced parameter identification algorithms and implement the strategy in experiments.

VI. ACKNOWLEDGEMENT

The research work is supported by NSF grants CMMI-1917300 and RINGS-2148353.

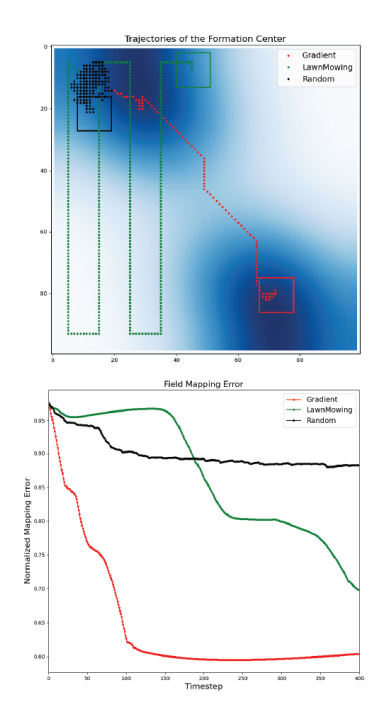


Fig. 5. The trajectories of the formation center following three different paths.

REFERENCES

- [1] D. Ucinski, Optimal measurement methods for distributed parameter system identification. CRC press, 2004.
- [2] H. T. Banks and K. Kunisch, Estimation techniques for distributed parameter systems. Springer Science & Business Media, 2012.
- [3] H. M. La, W. Sheng, and J. Chen, "Cooperative and active sensing in mobile sensor networks for scalar field mapping," *IEEE Transactions on Systems, Man, and Cybernetics: Systems*, vol. 45, no. 1, pp. 1–12, 2014
- [4] M. A. Demetriou, "Guidance of mobile actuator-plus-sensor networks for improved control and estimation of distributed parameter systems," *IEEE Transactions on Automatic Control*, vol. 55, no. 7, pp. 1570–1584, 2010
- [5] M. Patan, Optimal sensor networks scheduling in identification of distributed parameter systems. Springer Science & Business Media, 2012, vol. 425.
- [6] J. You and W. Wu, "Online passive identifier for spatially distributed systems using mobile sensor networks," *IEEE Transactions on Control Systems Technology*, vol. 25, no. 6, pp. 2151–2159, 2017.
- [7] M. A. Demetriou, "Adaptive techniques for the online estimation of spatial fields with mobile sensors," *IEEE Transactions on Automatic* Control, 2022.
- [8] Z. Zhang, S. T. Mayberry, W. Wu, and F. Zhang, "Distributed cooperative kalman filter constrained by advection-diffusion equation for mobile sensor networks," *Frontiers in Robotics and AI*, vol. 10, p. 1175418, 2023.
- [9] J. You, Z. Zhang, F. Zhang, and W. Wu, "Cooperative filtering and parameter identification for advection–diffusion processes using a mobile sensor network," *IEEE Transactions on Control Systems Technology*, vol. 31, no. 2, pp. 527–542, 2022.
- 10] J. You and W. Wu, "Sensing-motion co-planning for reconstructing a spatially distributed field using a mobile sensor network," in 2017 IEEE 56th Annual Conference on Decision and Control (CDC). IEEE, 2017, pp. 3113–3118.
- [11] —, "Geometric reinforcement learning based path planning for mobile sensor networks in advection-diffusion field reconstruction," in 2018 IEEE Conference on Decision and Control (CDC). IEEE, 2018, pp. 1949–1954.
- [12] D. Talwar, "Deep reinforcement learning based path-planning for multiagent systems in advection-diffusion field reconstruction tasks," 2020.
- [13] F. Zhang and N. E. Leonard, "Cooperative filters and control for cooperative exploration," *IEEE Transactions on Automatic Control*, vol. 55, no. 3, pp. 650–663, 2010.